Pyrolysis-Catalytic Steam Reforming/Gasification of Waste Tires for Production of Carbon Nanotubes and Hydrogen

Yeshui Zhang [a], Chunfei Wu [b*], Mohamad A. Nahil [a], Paul Williams [a*]

[a] Energy Research Institute, University of Leeds, Leeds, LS2 9JT, UK

(Tel: #44 1133432504; Email: p.t.williams@leeds.ac.uk)

[b] Department of Chemical Engineering, University of Hull, Hull, HU6 7RX, UK

(Tel: #44 1482466464; Email: c.wu@hull.ac.uk)

Abstract

The production of high-value carbon nanotubes and hydrogen from the two-stage pyrolysis catalytic-steam reforming/gasification of waste tires have been investigated. The catalysts used were Co/Al_2O_3, Cu/Al_2O_3, Fe/Al_2O_3 and Ni/Al_2O_3. The pyrolysis temperature and catalyst temperature were 600 °C and 800 °C, respectively. The fresh catalysts were analysed by temperature programmed reduction and X-ray diffraction. The product gases, including hydrogen were analysed by gas chromatography and the carbon nanotubes characterized by scanning and transmission electron microscopy and Raman spectrometry. The results showed that the Ni/Al_2O_3 catalyst produced high quality multiwalled carbon nanotubes along with the highest H_2 yield of 18.14 mmol g^{-1} tire, compared with the other catalysts, while the Co/Al_2O_3 and Cu/Al_2O_3 catalysts produced lower hydrogen yield, which is suggested to be associated with the formation of amorphous type carbons on the surface of the Co/Al_2O_3 and Cu/Al_2O_3 catalysts.

Key words: Pyrolysis, Plastics, Carbon nanotubes, Hydrogen, Catalysis

1 INTRODUCTION

Large quantities of waste tires are produced annually worldwide, for example, recent data report, 3.27 x 10^6 tonnes of waste tires arising in the Europe Union,[1] 3.87 x 10^6 tonnes in the US [2] and 1.01 x 10^6 tonnes in Japan. [3] Most developed countries have prohibited the disposal of waste tires to landfill, [4,5] because of their chemical and biological resistance to degradation. In addition, waste tires have a relatively high energy value (~32 $MJKg^{-1}$), and landfilling represents a waste of resource.

The treatment of waste tires is mainly through energy recovery options such as waste derived fuel in power stations, cement kilns and co-incineration, or through materials recycling such as rubber crumb for flooring, sports fields, roofing etc. [1] However, there is growing interest in other technologies and pyrolysis/gasification of waste tires has become a promising technology that has been extensively studied. [6-10] In addition, several reports have investigated the production of hydrogen from tire gasification.[11-13] Hydrogen is regarded as a clean energy carrier which is predicted to play a significant part in future energy scenarios, since it can be produced from many different sources, its combustion is pollutant free and it has a broad range of applications.[14]

Catalysts are normally used to enhance hydrogen production.[15-18] For example, Elbaba et al.[6, 11, 19, 20] used a two stage reaction system for hydrogen production from pyrolysis-catalytic gasification of waste tires. They investigated nickel based catalysts doped with other metals, for example the addition of cerium as a catalyst promoter produced high gas concentrations of hydrogen.[6] Process parameters have also been shown to influence hydrogen production from waste tires; for example, hydrogen production increased when catalyst temperature, catalyst/tire ratio, water injection rate and input of water (without excessive water) were increased.[19] Portofino et al.[13] also concluded that catalysts play an important role in the enhancement of hydrogen production in the gasification process. However catalyst deactivation derived from the formation of carbonaceous

coke on the catalyst surface is one of the challenges for optimising hydrogen production.[21-23] Giannakeas et al.[24] reported evidence from XRD analysis to showed that there was carbon deposition on the surface of the catalyst which caused catalyst deactivation in the waste tire reforming process. Coke formation on the catalyst surface during the reforming process is difficult to avoid and decreases the efficiency of the reforming process by deactivation of the catalyst. [25, 26] There are different forms of carbons generated in the coke deposition process, including amorphous carbons and graphitic carbons. Research into the types of carbon formed on the catalyst produced in the process of pyrolysis-catalytic gasification for hydrogen production using plastics have reported that some of the graphitic carbons have been shown to be carbon nanotubes (CNTs) [27, 28] and can be regarded as a valuable by-product, instead of being considered as un-wanted coke. Therefore there is interest in trying to manipulate the process by the use of different catalysts to optimize the production of CNTs and/or hydrogen.

Carbon nanotubes have special physical and chemical properties which enable their use in many application areas. For example; bulk CNTs have been used for rechargeable batteries, automotive parts and in sporting goods; [29,30] CNTs can also be used as multifunctional coating materials, for example, multi-walled carbon nanotubes (MWNTs) can be added into paint which can discourage reduce bio-fouling;[29, 31] MWNTs have been used widely in lithium ion batteries [29, 32, 33] where they have been shown to improve the electrical and mechanical properties of batteries [29, 34, 35] CNTs also be used in biosensors and medical devices because of their chemical and dimensional compatibility with biomolecules.[29, 36]

Although noble metals are the most effective catalysts to promote hydrogen production,[15,16] they are not the ideal catalysts for large scale industrial use due to their higher cost. Therefore, there has been much research into the use of other metal-based catalysts for hydrogen production. For example Patel et al.[37] and Marino et al. [38] used Cu based catalysts and Zhang et al.[39] used Co based catalysts to investigate their influence on the ethanol reforming process. Ni-based catalysts have

been used for the pyrolysis-catalytic reforming/gasification of plastic wastes, tires and refuse derived fuel for hydrogen production.[11, 40-41] Cu based catalysts have been shown to promote hydrogen production in a waste tire pyrolysis process.[42] Metal-based catalyst have also been used for the enhanced production of carbon nanotubes. For example, Qian et al.[43] used a Co based catalyst in a methane decomposition process to enhance CNTs production and Yu et al.[44] investigated the influence of a Fe-Mo/Al_2O_3 catalyst on CNTs production in the catalytic pyrolysis of propylene.

To our best knowledge, there are limited reports in relation to the co-production of hydrogen and CNTs from the pyrolysis-catalytic reforming of waste tires, although, there have been reports regarding the simultaneous production of H_2 and CNTs from waste plastics. [27, 28] In this paper we report on a study of four metal-based catalysts using Al_2O_3 as catalyst support, to determine which metal-based catalyst was most effective for co-production of CNTs and hydrogen from the catalytic reforming of waste tire.

2 MATERIALS AND METHODS

2.1 Experimental System

Experiments were undertaken using a two stage fixed-bed, pyrolysis-catalytic reforming/gasification reactor shown in Figure 1. The reactors were constructed of stainless steel and were externally electrically heated with furnaces with full temperature control and monitoring. Pyrolysis of the waste tire occurred in the first reactor at 600 °C and the product pyrolysis volatiles were passed directly to the second rector, where catalytic reforming in the presence of steam occurred at 800 °C. Nitrogen was introduced into the top of the pyrolysis reactor as the inert purge gas with a flow rate of 80 ml min^{-1}. The tire sample (around 1 g) was placed in the pyrolysis reactor

and the catalyst or sand (around 0.5 g) was located in the second reactor. During the experiments, the catalyst bed (second reactor) was preheated at 800 °C before the pyrolysis of the tire was started heating from room temperature to 600 °C with a heating rate of 40 °C min^{-1}. The gaseous products from the process were passed to two water and solid-CO_2 cooled condensers to trap the condensable liquids followed by gas collection in a 25L Tedlar^{TM} gas sample bag. The total experimental time was around 40 min, and the gas collection time was around 60 min (extra time was used to ensure all the products were collected).

2.2 Materials

The waste tire sample used in the experiments was a shredded mixture of waste truck tires. The sample was prepared by removing the steel and shredding into particles of ~6 mm. The elemental analysis of the tires was carbon, 81.2 wt.%, hydrogen 7.2 wt.%, nitrogen 0.8 wt.% and sulphur 2.1 wt.% determined using a Carlo Erba Flash EA1112 elemental analyser. Proximate analysis of the tire showed 0.82 wt.% of moisture, 62.7 wt.% of volatiles, 32.31 wt.% of fixed carbon and 4.17 wt.% of ash.

The four catalysts investigated, Fe/Al_2O_3, Cu/Al_2O_3, Co/Al_2O_3 and Ni/Al_2O_3 were prepared by an incipient wetness method. The metals were impregnated onto an alumina support to produce 10 wt.% of metal catalyst. Firstly, the metal nitrates were dissolved in ethanol, alumina was added into the metal nitrate and ethanol mixture with continuous stirring to produce a slurry. The precursor slurry was dried in an oven at 50 °C for around 12 h until all of the excess ethanol was evaporated. The dried catalyst precursor was calcined by heating in air to a final temperature of 750 °C with a heating rate of 2 °C min^{-1} and held at 750 °C for 3 hours. The catalyst was ground and sieved to a size range between 0.05 and 0.18 mm.

2.3 Analytical Methods

The gaseous product from the pyrolysis-catalytic reforming/gasification process collected by the Tedlar gas sample bag was analysed by packed column gas chromatography (GC). Permanent gases which included H_2, CO, O_2, and N_2 were analysed by a Varian 3380 gas chromatograph fitted with a thermal conductivity detector with a 2 m long x 2 mm diameter, 60-80 mm mesh molecular sieve column. CO_2 was analysed on the same GC, but with a separate 2 m long x 2 mm diameter column with HayeSep 80-100 mesh molecular sieve and a thermal conductivity detector. The carrier gas was argon. Hydrocarbons from C_1-C_4 were determined using a separate Varian 3380 GC with a 80-100 mesh HayeSep column, with nitrogen carrier gas and a flame ionization detector.

Temperature programmed oxidation (TPO) used a Shimadzu thermo gravimetric analyser (TGA) to determine the oxidation characteristics of carbon deposited on the catalyst after use to identify the formation and type of deposited carbon on the surface. Approximate 4 mg of the reacted catalyst sample was placed in the TGA and heated in air at a flow rate of 50 ml min^{-1}. The sample was heated to 800 °C at a heating rate of 15 °C min^{-1}.

Temperature programmed reduction (TPR) of the fresh catalysts was carried out using a Stanton-Redcroft thermo gravimetric analyser (TGA). 4 mg of the catalyst was preheated to 150 °C at a heating rate is 20 °C min^{-1} and held for 30 min in an atmosphere of H_2 (5 vol.% balanced with N_2) at a flow rate of 50 ml min^{-1}, the sample was then heated to 900 °C at a heating rate of 10 °C min^{-1}.

The fresh catalysts and used catalysts after experimentation were characterized by scanning electron microscopy (SEM) and transmission electron microscopy (TEM) to determine their surface morphology. The SEM used was a Hitachi SU8230 SEM and the TEM was a FEI Tecnai TF20). The bulk crystal structure and chemical phase composition of the catalysts was determined by X-ray

diffraction using a Phillips PW 1050 Goniometer with a CU Ka radiation X-ray tube operated at 40 kV and 40 mA.

The catalysts after experimentation contained deposited carbonaceous coke which was characterised by Raman spectroscopy using a Renishaw Invia Raman spectrometer at a wavelength of 514 nm at Raman shifts between 100 and 3200 cm^{-1}. The analysis was able to investigate the graphitic nature of the deposited carbon.

3 RESULTS AND DISCUSSION

3.1 Characterisation of the fresh catalysts

Figure 2 shows scanning electron micrographs of the fresh catalysts and show that the surface structures of the catalysts are composed of many irregular particles. Temperature programmed reduction of the catalysts (Figure 3) showed that Ni/Al_2O_3 had two main reduction peaks which appeared at temperatures of around 230 and 800 °C which may be assigned to the reduction of bulk NiO particles and Ni-Al spinel phases ($NiAl_2O_4$), respectively. The presence of NiO and $NiAl_2O_4$ phases were reported by Wu et al. [45] and Clause et al. [46] There were several reduction peaks for the Fe/Al_2O_3 catalyst, which may be due to the reduction of Fe_2O_3 to Fe_3O_4, Fe_3O_4 to FeO, and FeO to Fe. The relatively low temperature reduction is related to the well dispersed iron on the support. [47] Brown et al. [48] suggested the reduction peak of Fe_3O_4 to FeO were related to partial reduction and re-oxidation. Wan et al.[49] described the reduction of Fe_2O_3 as being to FeO, a metastable phase, rather than to Fe which oxides below 570 °C. Berry et al. [50] found the reduction of Fe_2O_3 to Fe occurred at around 440 and 640 °C which are similar to the result in Figure 3, the reduction peaks at 460 and 630 °C respectively. The reduction peak for the Fe-Al spinel phase is at a relatively high

temperature, which has been reported to be due to the strong interaction between iron and the alumina support. [48]

The Cu/Al_2O_3 catalyst had two main reduction stages at 210 and 300 °C, respectively; it is noted that a broad slow reduction was observed for the TPR analysis of the Cu/Al_2O_3 catalyst at temperatures between 300 and 700 °C. The first reduction peak indicates the presence of CuO and the second peak is assigned to the reduction of $CuAl_2O_4$. Marino et al. [51] have reported the presence of both of CuO and $CuAl_2O_4$ phases in Cu/Al_2O_3 catalyst.

For the Co/Al_2O_3 catalyst, it appears that this catalyst is hardly reduced under the TPR conditions used, suggesting that there were limited active Co sites in this catalyst. The result is similar to that reported by Chu et al.[52] who found no Co_3O_4 component for a cobalt-alumina supported catalyst.

3.2 Pyrolysis-catalytic reforming/gasification of waste tires

3.2.1. Mass balance and hydrogen production

Pyrolysis-catalytic reforming/gasification of the waste tires was carried out using the different metal based catalysts and the resultant mass balance data and gas concentrations are shown in Table 1. The standard deviation for mass balance and hydrogen production using Ni/Al_2O_3 were 3.75 and 4.10, respectively. The product yields including gas, liquid and residue yields were calculated in relation to the mass of the waste tires. The liquid and residue yields were obtained by mass difference before and after experimentation and the gas yield was calculated based on the gas concentration from gas chromatography analysis and the molecular mass of the individual gases to calculate the mass of gas. Hydrogen sulphide which would be produced from the sulphur in the tire was not analysed in this work. The mass balance and carbon (wt.%) were calculated using the

weight of products divided by the weight of tire sample (as shown in Equation 1); the calculation of carbon yield is shown in Equation 2.

$$\text{Mass balance (wt.\%)} = \frac{\text{weight of (resiude + gas + carbon + liquid)}}{\text{weight of tire}} \times 100 \text{ (Equation 1)}$$

$$Carbon\ yield\ (wt.\%) = \frac{Weight\ differen\ of\ the\ catalytic\ reactor}{Weight\ of\ tire} \times 100\ (Equation\ 2)$$

Table 1 shows that for the four investigated catalysts, the total gas yield ranking from the pyrolysis-catalytic reforming/gasification process was Ni/Al_2O_3 > Cu/Al_2O_3 > Fe/Al_2O_3 > Co/Al_2O_3. The ranking of liquid yield in the reforming process was Co/Al_2O_3 > Ni/Al_2O_3 > Cu/Al_2O_3 > Fe/Al_2O_3. The residue yield for pyrolysis using different catalysts remained constant at ~38 wt.% which was expected since the pyrolysis process which generates the solid char (and ash) residue is separated from the catalytic stage.

The highest hydrogen production for the pyrolysis-catalytic reforming/gasification of the waste tires was with the Ni/Al_2O_3 catalyst, increasing from 4.96 mmol g^{-1} tire when sand was used to 18.14 mmol g^{-1} tire for the Ni/Al_2O_3 catalyst., The hydrogen yields are much lower with other catalysts which were 9.03 mmol g^{-1} tire with the Co/Al_2O_3 catalyst, 7.26 mmol g^{-1} tire with the Fe/Al_2O_3 catalyst and 5.53 mmol g^{-1} tire with the Cu/Al_2O_3 catalyst (Table 1). Portofino and co-authors [13] found that a nickel based catalyst had a significant effect in the waste tire catalytic reforming process, by significantly increasing hydrogen production. They also reported that a Ni/Al_2O_3 catalyst resulted in the highest production of hydrogen whereas a Cu/Al_2O_3 catalyst gave a relatively low yield of hydrogen.

In this work, the total yield of carbon was calculated as the weight increase of the catalytic reactor tube compared to the weight of tire sample and represented carbon deposition on the catalyst and in the reactor tube. The ranking of carbon yield was Cu/Al_2O_3) = Fe/Al_2O_3 > Ni/Al_2O_3 > Co/Al_2O_3.

Unlike other work investigating tire gasification where steam is usually introduced into the process, in this work, steam could only be generated from the internal moisture content of the tire sample. Therefore, steam reforming reactions (Reaction 1) would be limited in our process. In addition, carbon deposition on the surface of the catalyst would be enhanced by the lower steam presence, since the carbon steam reaction (Reaction 2) would be depressed.[53] Carbon formation in the presence of the different catalysts is suggested to be related to Reaction 3; and both Reaction 3 (hydrocarbon decomposition) and Reaction 4 (water gas shift reaction) which are suggested to be responsible for hydrogen production from the tire gasification process.

$$C_nH_m + 2H_2O \rightarrow nCO + \left(n + \frac{m}{2}\right)H_2 \qquad \text{(Reaction 1)}$$

$$C + H_2O \rightarrow CO + H_2 \qquad \text{(Reaction 2)}$$

$$C_nH_mO_z \rightarrow zCO + (n - z)C + H_2 \qquad \text{(Reaction 3)}$$

$$CO + H_2O \rightarrow CO_2 + H_2 \qquad \text{(Reaction 4)}$$

3.2.2. Carbon deposition on the catalysts

Figure 4 shows the temperature programmed oxidation (TPO) results for the Fe/Al_2O_3, Cu/Al_2O_3, Co/Al_2O_3 and Ni/Al_2O_3 catalysts after use in the pyrolysis-catalytic reforming/gasification of waste tire process. For the used Cu/Al_2O_3 catalyst, there was a slight weight increase in mass at around 400 °C, which was attributed to the oxidation of Cu metal, which is suggested to be reduced from copper oxides during the pyrolysis process where reducing agents e.g. CO and H_2 were produced. The result is consistent with the temperature programmed reduction analysis of the fresh Cu/Al_2O_3 (Fig. 3), which showed the largest reduction peak at the lowest reduction temperature (~210 ˚C) compared with the other catalysts.

From the weight loss data from the TPO analysis of the used catalysts from the processing of the waste tires, the mass of carbon on the catalyst could be determined. The results showed that around 15 wt.% of the weight of the reacted catalysts were ascribed to the deposited carbon. The oxidation of the carbon resulting in weight loss at a temperature of around 550 °C was attributed to the oxidation of amorphous carbons, while the oxidization at around 650 °C was attributed to the oxidation of filamentous carbons. [54] The derivative-temperature programmed oxidation results (DTG-TPO) of the used Co/Al_2O_3, Fe/Al_2O_3, Cu/Al_2O_3 and Ni/Al_2O_3 catalysts are shown in Figure 5. The DTG-TPO results of the used Co/Al_2O_3 and Cu/Al_2O_3 catalysts show that two main oxidation peaks are observed indicating there are two different types of carbons despoisted on to the catalyst surface during the process. Two oxidation peaks, at temperatures of ~500 °C and ~600 °C, were obtained from the DTG-TPO analysis for both the Co/Al_2O_3 and Cu/Al_2O_3 catalysts, suggesting that both amorphous and filamentous carbons are formed with these catalysts. However, for the used Fe/Al_2O_3 and Ni/Al_2O_3 catalysts, there was only one peak at a temperature of ~600 °C identified by DTG-TPO (Figure 5), suggesting that the deposited carbon was mainly graphitic filamentous carbons. The DTG-TPO results for the used Ni/Al_2O_3 catalyst showed the highest oxidation temperature at ~635 °C for carbon oxidation (Figure 5) also showing a high production of mainly filamentous carbons for the Ni-based catalyst.

Scanning electron microscopy (SEM) was also used to examine the used catalysts from the pyrolysis-catalytic reforming/gasification of waste tire and the micrographs are shown in Figure 6. Figure 6(a) showed that almost no filamentous carbons could be seen on the surface of the reacted Co/Al_2O_3 catalyst. The results were consistent with the temperature programmed oxidation analysis (Figure 5) where amorphous carbons were suggested to be the main carbons formed on the reacted Co/Al_2O_3 catalyst. In addition, only a small amount of filamentous carbons could be observed from the Figure 6(b) for the reacted Cu/Al_2O_3 catalyst. However, Figure 6(c) and 6(d), show that filamentous carbons were widely distributed on the surface of the used Fe/Al_2O_3 and Ni/Al_2O_3

catalysts. The filamentous carbon produced on the surface of the used Ni/Al_2O_3 catalyst were relatively long (Figure 6(d)) compared with filamentous carbons formed using the other catalysts. Transmission electron microscopy (TEM) analysis of the used catalyst was also carried out. The results shown in Figure 7(a) and 7(b) confirm that no filamentous carbons were found for the Co/Al_2O_3 or Co/Al_2O_3 catalysts however, the filamentous carbons which were abundant for the Ni/Al_2O_3 catalyst (Figure 6(d)) are shown by the TEM analysis (7(d) to be multi-walled carbon nanotubes (MWCNTs). The Ni/Al_2O_3 catalyst produced the CNTs that were relatively long and smooth. The SEM and TEM results are consistent with the TPO and DTG-TPO analysis (Figure 4 and Figure 5) where carbons produced from the Ni/Al_2O_3 catalyst have the highest fraction of filamentous carbons. The Fe/Al_2O_3 catalyst produced carbons with a mainly filamentous structure, and indistinct disrupted nanotube structure (Figure 7(c).

Raman spectroscopy analysis was used to characterize the carbons formed using the different catalysts during the pyrolysis-catalytic reforming/gasification process for waste tires and the results are shown in Figure 8**.** The D band at the Raman shift around wavelength 1352 cm^{-1} indicates amorphous or disordered carbons. The G band at the Raman shift around wavelength 1587 cm^{-1} indicates a graphite carbon structure. The second order Raman spectrum G` at the Raman shift around wavelength 2709 cm^{-1} indicates the two photon elastic scattering process. [55, 56] The carbon materials produced in this work have similar Raman shift patterns compared with CNTs produced from other work and commercial CNTs. [57-59] To evaluate the degree of graphitization of the CNTs produced from the waste tires, the intensity of the D band (I_D) normalized to the intensity of the G band (I_G), the I_D/I_G ratio is used. The carbons from the Ni/Al_2O_3 catalyst showed a relatively low D/G ratio compared with the Co/Al_2O_3, Cu/Al_2O_3 and Fe/Al_2O_3 catalysts, indicating that the carbons produced with these catalysts are less disordered and containing less amorphous carbons. The results are consistent with the TPO, SEM and TEM analysis, indicating that the Ni/Al_2O_3 catalyst was the best catalyst for CNTs production in terms of crystallization, smooth surface

morphologies and yield. The relatively low I_D/I_G ratio for the carbon deposited on the Ni/Al_2O_3 catalyst also indicates the relatively high quality of the CNTs produced with less structural defects.[57, 58, 60, 61]

4 CONCLUSIONS

In this study, four different kinds of catalysts (Co/Al_2O_3, Cu/Al_2O_3, Fe/Al_2O_3 and Ni/Al_2O_3) were investigated for the pyrolysis-catalytic reforming/gasification of waste tires for the production of hydrogen and high-value carbon nanotubes. The results suggested that;

1) The presence of catalysts can enhance the waste tire pyrolysis reforming/gasification process to produce higher yields of gas and hydrogen production. The Ni/Al_2O_3 catalyst gave the highest gas yield and the highest H_2 production;
2) The Ni/Al_2O_3 catalyst gave the highest quality of CNTs production along with a relatively high yield of product gas from the pyrolysis-catalytic reforming/gasification process. SEM results showed the carbon deposits to be relatively long, straight and of regular shape and TEM analysis confirmed that the filamentous carbons were multi-walled carbon nanotubes. Raman spectrometry analysis showed the highest purity of CNTs were produced from the Ni/Al_2O_3 catalyst, compared to the Co/Al_2O_3, Cu/Al_2O_3 and Fe/Al_2O_3 catalysts.

REFERENCES

[1] European Tyre & Rubber Manufactureres' Association, ELT Management, ETRMA, 2014.

[2] Rubber Manufacturers Association, 2011 U.S.Scrap Tire Market Summary, 2001.

[3] Tyre Industry of Japan 2013, JATMA, Japan Automobile Tyre Manufacturers Association, Tokyo, Japan, 2013.

[4] European Commission- Environment, Landfill of Waste, European Commission, Brussels, 2014.

[5] Environmental Protection Agency, Waste-Resource Conservation-Common Wastes & Materials-Scrap Tires, Environmental Protection Agency, Washington, 2012.

[6] Elbaba, I.F.; Wu, C.; Williams, P.T. Int. J. Hydrogen Energy, **2011**, *36*, 6628-6637.

[7] Leung, D.Y.C.; Wang, C.L. Fuel Proc. Technol., **2003**, *84*, 175-196.

[8] Xiao, G.; Ni M.J.; Chi, Y. Cen, K.F. Energ. Convers. Manag. **2008**, *49* 2078-2082.

[9] Galvagno, S.; Casciaro, G.; Casu, S.; Martino, M.; Mingazzini, C.; Russo, A.; Portofino, S. Waste Manag. **2009**, *29*, 678-689.

[10] Williams, P.T.; Brindle, A.J. J. Anal. Appl. Pyrolysis, **2003,** *67*, 143-164.

[11] Elbaba, I.F.; Wu, C.; Williams, P.T. Energ. Fuel., **2010,** *24*, 3928-3935.

[12] Pattabhi Raman K.; Walawender, W.P.; Fan, L.T. Conserv. Recycl., **1981**, *4*, 79-88.

[13] Portofino, S.; Casu, S. Iovane, A.R.P.; Martino, M.; Donatelli, A.; Galvagno, S. Energ. Fuel., **2011**, *25* 2232-2241.

[14] Dell, R.M.; Moseley, P.T.; Rand, D.A.J. (Ed.) Towards Sustainable Road Transport, Academic Press, Boston, 2014.

[15] Mortola,V.B.; Damyanova, S.; Zanchet, D.; Bueno, J.M.C. Appl. Catal. B-Environ., **2011**, *107*, 221-236.

[16] Nishikawa, J.; Nakamura, K.; Asadullah, M.; Miyazawa, T.; Kunimori, K.; Tomishige, T. Catal. Today, **2008**, *131*, 146-155.

[17] Yung, M.M.; Jablonski, W.S.; Magrini-Bair, K.A. Energ. Fuel., **2009**, *23*, 1874-1887.

[18] Sehested, J. Catal. Today, **2006**, 1*11*, 103-110.

[19] Elbaba, I.F.; Williams, P.T. Appl. Catal. B-Environ., **2012**, *125*, 136-143.

[20] Elbaba, I.F.; Williams, P.T. Energ. Fuel., **2014**, *28*, 2104-2113.

[21] Trimm, D.L. Catal. Today, **1997**, *37*, 233-238.

[22] La Cava, A.I.; Bernardo, C.A.; Trimm, D.L. Carbon, **1982**, *20*, 219-223.

[23] Borowiecki, T. Appl. Catal., **1982**, *4*, 223-231.

[24] Giannakeas, N.; Lea-Langton, A.; Dupont, V. Twigg, M.V. Appl. Catal. B-Environ., **2012**, *126*, 249-257.

[25] Ebshish, A.; Yaakob, Z.; Taufiq-Yap, Y.H.; Bshish, A.; Tasirin, S.M. Proc. Instit. Mech. Eng., A: J. Power Energ., **2012**, *226*, 1060-1075.

[26] Avasthi, K.S.; Reddy, R.N.; Patel, S. Procedia Eng., **2013**, *51*, 423-429.

[27] Wu, C.; Nahil, M.A.; Miskolczi, N.; Huang, J.; Williams, P.T. Env. Sci. Technol., **2013**, *48*, 819-826.

[28] Wu, C.; Wang, Z.; Wang, L.; Williams, P.T.; Huang, J. RSC Adv., **2012**, *2*, 4045-4047.

[29] De Volder, M.F.L.; Tawfick, S.H.; Baughman, R.H.; Hart, A.J. Science, **2013**, *339*, 535-539

[30] Peng, B.; Locascio, M.; Zapol, P.; Li, S.; Mielke, S.L.; Schatz, G.C.; Espinosa, H.D., Nature Nano, **2008**, *3*, 626-631.

[31] Beigbeder, A.; Degee, P.; Conlan, S.L.; Mutton, R.J.; Clare, A.S.; Pettitt, M.E. M.E. Callow, M.E.; Callow, Dubois, P. Biofoul., **2008**, *24*, 291-302.

[32] Dai, L.; Chang, D.W.; Baek, J.B.; Lu, W. Small, **2012**, *8*, 1130-1166.

[33] Köhler, A.R.; Som, C.; Helland, A.; Gottschalk, F. J. Clean. Prod., **2008**, *16*, 927-937.

[34] Evanoff, K.; Khan, J.; Balandin, A.A.; Magasinski, A.; Ready, W.J.; Fuller, T.F.; Yushin, G. Adv. Mater., **2012**, *24*, 533-537.

[35] Sotowa, C.; Origi, G.; Takeuchi, M.; Nishimura, Y.; Takeuchi, K.; Jang, I.Y.; Kim, Y.J.; Hayashi, T.; Kim, Y.A.; Endo, M.; Dresselhaus, M.S. ChemSusChem, **2008**, *1*, 911-915.

[36] Heller B.S.; Baik, S.; Eurell, T.E.; Strano, M.S.; Adv. Mater., **2005**, *17*, 2793-2799.

[37] Patel, S.; Pant, K.K. J. Power Source., **2006**, *159*, 139-143.

[38] Mariño, F.; Boveri, M.; Baronetti, G.; Laborde, M. Int. J. Hydrogen Energy, **2004**, *29*, 67-71.

[39] Zhang, B.; Tang, X.; Li, Y.; Xu, Y.; Shen, W., Int. J. Hydrogen Energy, **2007**, *32*, 2367-2373.

[40] Wu C.; Williams P.T., Waste Resour. Manag., **2014**, *167*, 35-46

[41] Blanco, P.H.; Wu, C.; Onwudili, J.A.; Williams, P.T. Appl. Catal. B-Environ., **2013**, *134*, 238-250.

[42] Ke-Chang Q.C.X.; Bao, H.; W.R.; Wei, H.; Zhao, J.B., **2004**, *26*, 397-407.

[43] Qian, W.; Liu, T.; Wei, F.; Wang, Z.; Li, Y. Appl. Catal. A-Gen., **2004**, *258*, 121-124.

[44] Yu, Q.Z.H.; Wei, F.; Qian, W.; Luo, G. Carbon, **2003**, *41*, 2855-2863.

[45] Wu, C.; Williams, P.T. Appl. Catal. B-Environ., **2009**, *90*, 147-156.

[46] Clause, O.; Gazzano, M.; Trifiro′, F.; Vaccari, A.; Zatorski, L. Appl. Catal., **1991**, *73*, 217-236.

[47] Bukur, D.B.; K. Okabe, K.; Rosynek, M.P.; Li, C.P.; Wang, D.J.; Rao, K.R.P.M.; Huffman, G.P. J. Catal., **1995**, *155*, 353-365.

[48] Brown, R.; Cooper, M.E.; Whan, D.A. Appl. Catal., **1982**, *3*, 177-186.

[49] Wan, H.J.; Wu, B.S.; Zhang, C.H.; Xiang, H.W.; Li, Y.W.; Xu, B.F.; Yi, F. Catal. Comm., **2007,** *8*, 1538-1545.

[50] Berry, F.J.; Smart, L.E.; Prasad, P.S.; Lingaiah, N.; Rao, P.K. Appl. Catal. A-Gen., **2000**, *204*, 191-201.

[51] Mariño, F.J.; Cerrella, E.G.; Duhalde, S.; Jobbagy, M.; Laborde, M.A. Int. J. Hydrogen Energy, **1998**, *23*, 1095-1101.

[52] Chu, W.; Chernavskii, P.A.; Gengembre, L.; Pankina, G.A.; Fongarland, P.; Khodakov, A.Y. J. Catal., **2007**, *252*, 215-230.

[53] Gašparovič L.; Šugár L.; Jelemenský L.; Markoš J. Chem. Pap. **2013**, *67*, 1504

[54] Wu C.; Williams P.T. Appl. Catal. B-Environ., **2010**, *96*, 198-207.

[55] Wu, C.; Wang, Z.; Williams, P.T.; Huang, J. Sci. Rep., **2013**, *3*, 2742; DOI:10.1038/srep02742

[56] Dresselhaus, M.S.; Dresselhaus, G.; Jorio, A.; Souza Filho, A.G. Saito, R. Carbon, **2002**, *40*, 2043-2061.

[57] Popovska, N.; Danova, K.; Jipa, I.; Zenneck, U. Powder Technol., **2011**, *207*, 17-25.

[58] Weizhong, Q.; Fei, W.; Zhanwen, W.; Tang, L.; Hao, Y.; Guohua, L.; Lan, X. Xiangyi, D. AIChE J., **2003**, *49*, 619-625.

[59] See, C.H.; Dunens, O.M.; MacKenzie, K.J.; Harris, A.T. Ind. Eng. Chem. Res., **2008,** *47*, 7686-7692.

[60] Triantafyllidis, K.S.; Karakoulia, S.A.; Gournis, D.; Delimitis, A.; Nalbandian, L.; Maccallini, E.; Rudolf, P. Micropor.. Mesopor. Mat., **2008**, *110*, 128-140.

[61] Porwal, D; Mukhopadhyay, K.; Ram, K.; Mathur, G.N. Thermochim. Acta, **2007**, *463*, 53-59.

Table 1 Mass balance and gas concentrations for the pyrolysis-catalytic gasification of tire

	Sand	Fe/Al_2O_3	Cu/Al_2O_3	Co/Al_2O_3	Ni/Al_2O_3
Gas yield (wt.%)	30.26	22.07	30.40	24.76	34.60
Liquid yield (wt.%)	18.00	11.00	14.00	24.00	20.00
Residue (wt.%)	38.00	38.00	36.00	37.00	39.00
Hydrogen production (mmol g^{-1} tire)	4.96	7.26	5.53	9.03	18.14
Carbon (wt.%)	-	14.00	14.00	8.00	12.00
Mass balance (wt.%)	86.26	92.43	94.40	93.76	105.60
Gas concentrations (vol.%)					
CO	3.04	7.83	3.30	12.80	16.06
H_2	23.79	33.12	25.38	46.20	57.47
CH_4	63.23	51.62	64.29	30.44	19.66
CO_2	1.29	1.11	1.34	1.69	1.07
C_2	8.51	5.74	5.20	8.78	4.01
C_3	0.14	0.09	0.06	0.10	0.04
C_4	0.00	0.48	0.42	0.00	0.35

Figure Captions

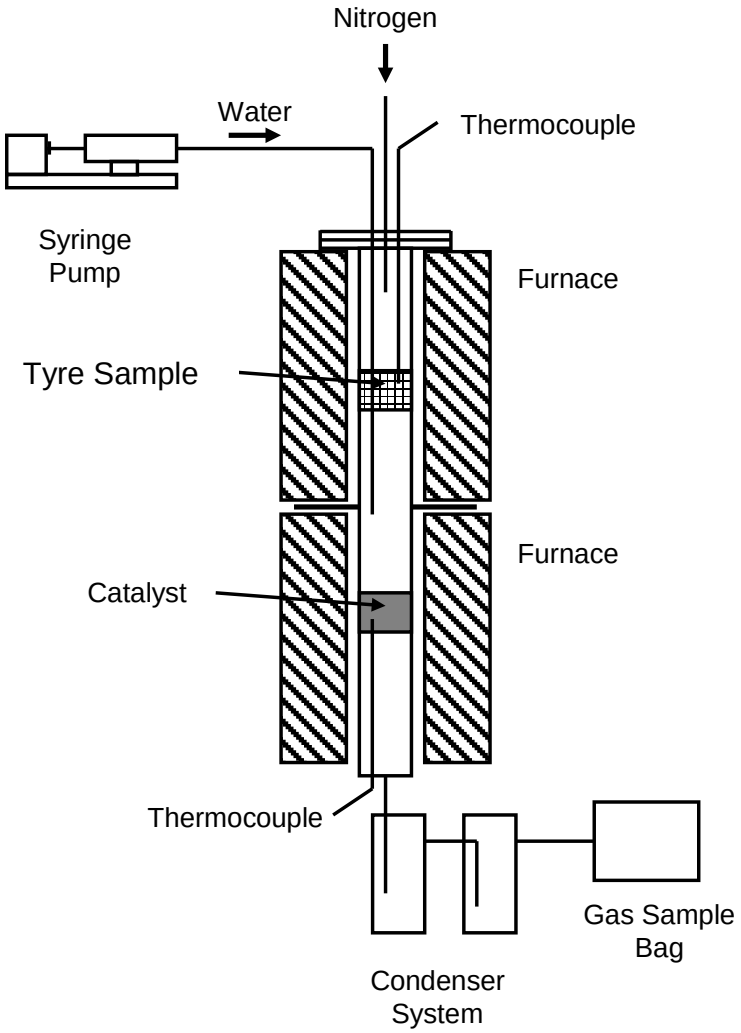

Figure 1. Schematic diagram of the pyrolysis-catalytic gasification reactor system

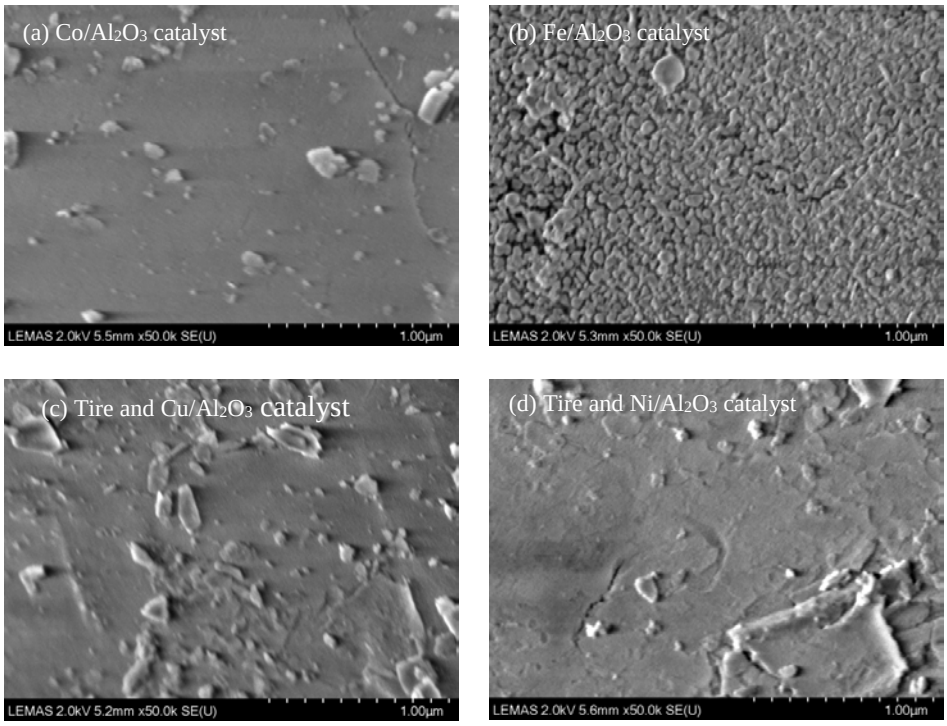

Figure 2 SEM analysis of fresh catalyst before pyrolysis-catalytic gasification of waste tire

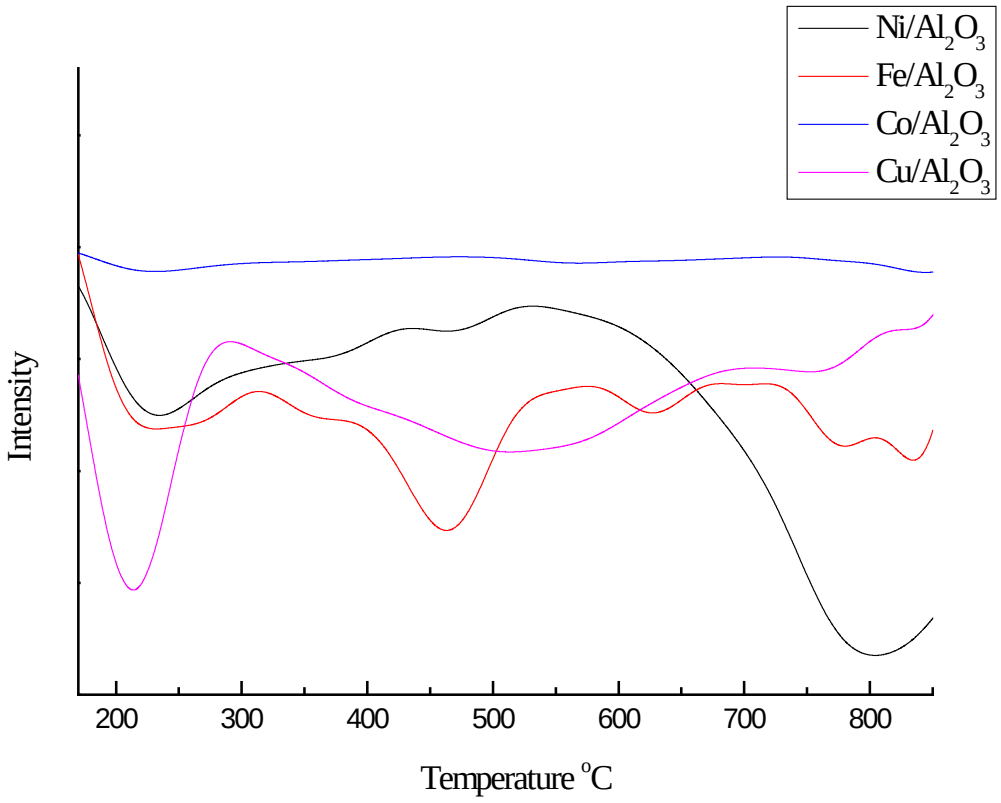

Figure 3 DTG-TPR results of different fresh catalysts

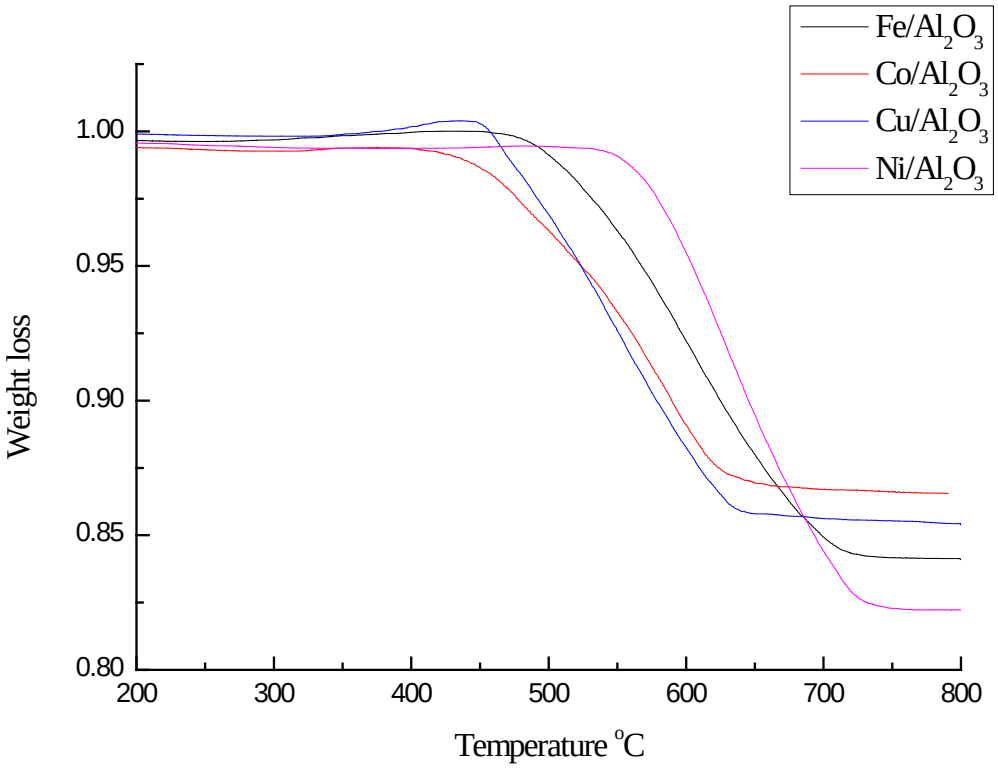

Figure 4 TPO results of different reacted catalysts from the pyrolysis-catalytic tire gasification

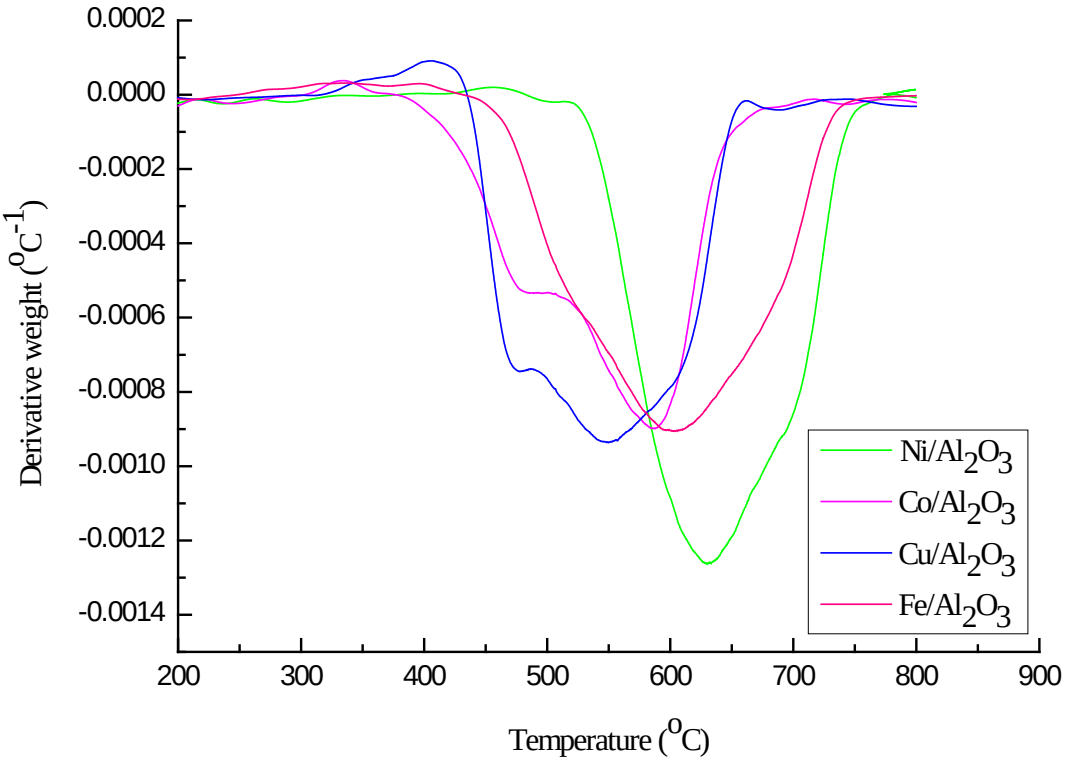

Figure 5 DTG-TPO results of different reacted catalysts from the pyrolysis-catalytic tire gasification

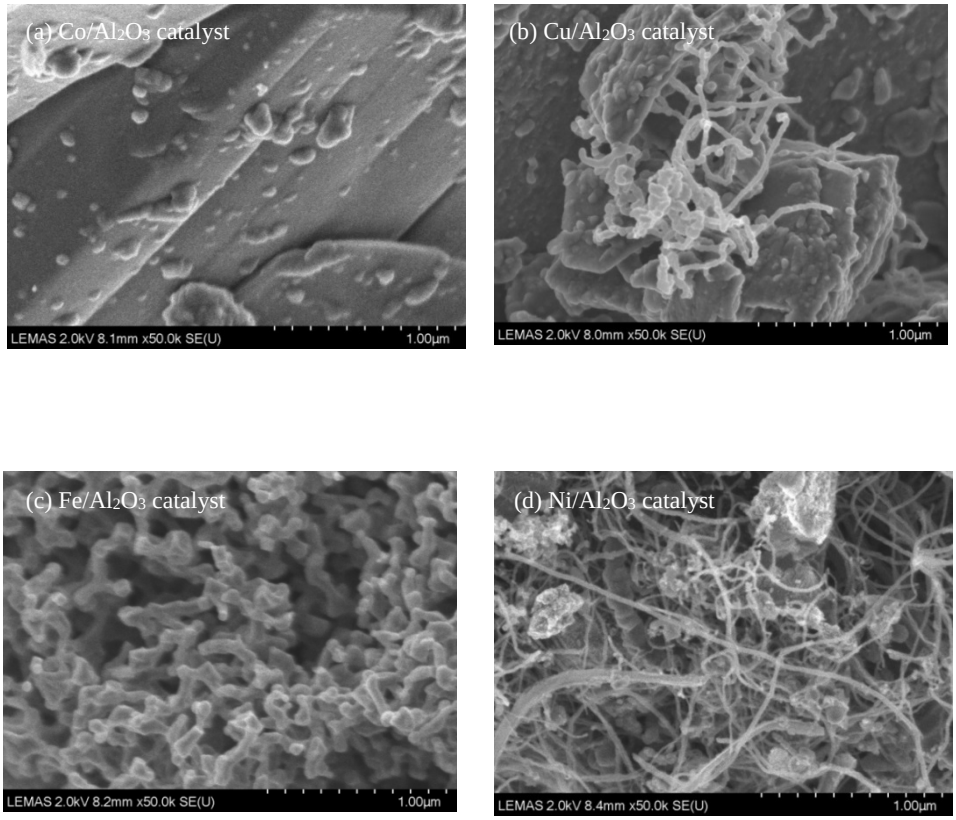

Figure 6 SEM analysis of the reacted Co/Al_2O_3, Cu/Al_2O_3, Fe/Al_2O_3 and Ni/Al_2O_3 catalysts after the pyrolysis-gasification of waste tire

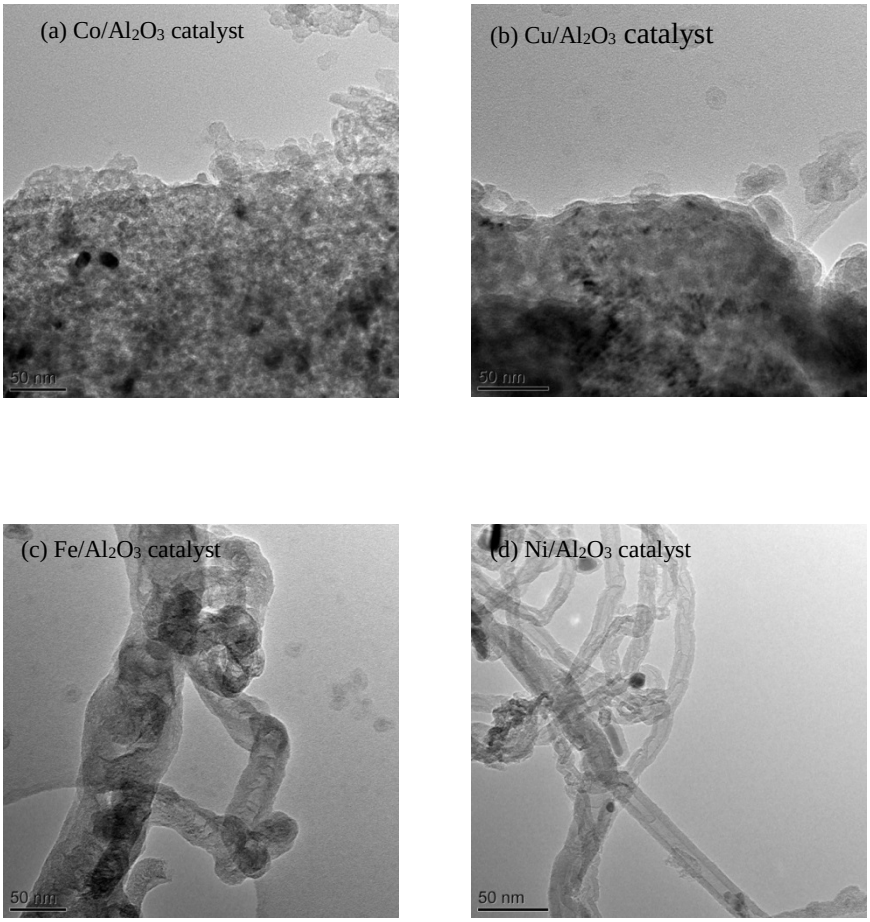

Figure 7 TEM analysis of the reacted Co/Al_2O_3, Cu/Al_2O_3, Fe/Al_2O_3 and Ni/Al_2O_3 catalysts derived from pyrolysis-gasification of waste tire

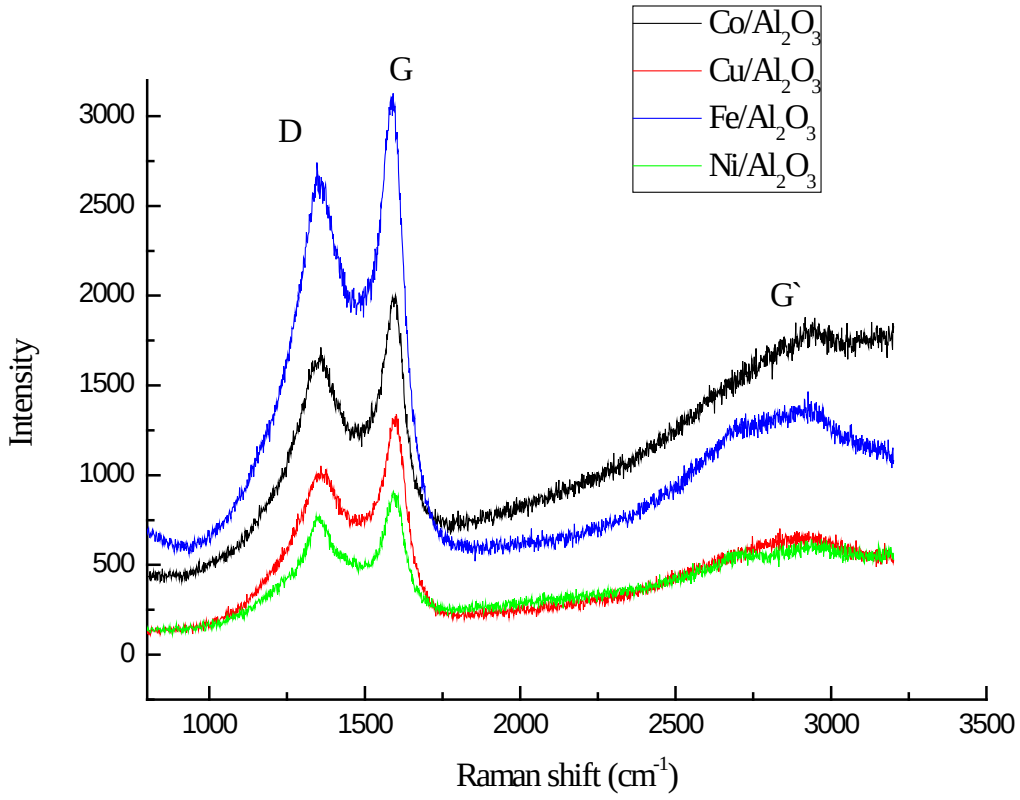

Figure 8 Raman analysis of the 4 reacted catalysts (Fe/Al_2O_3, Cu/Al_2O_3, Co/Al_2O_3, Ni/Al_2O_3)